Journal of the European Ceramic Society 17 (1997) 513–523

PII: S0955-2219(96)00096-9
0955-2219/97/$17.00

ZnO-Doped $BaTiO_3$: Microstructure and Electrical Properties

A. C. Caballero,* J. F. Fernández,† C. Moure & P. Durán

Electroceramics Department, Instituto de Cerámica y Vidrio (CSIC), Carretera de Valencia km. 24,300, 28500 Arganda del Rey, Madrid, Spain

(Received 6 March 1996; revised version received 16 May 1996; accepted 21 May 1996)

Abstract

In the present work, ZnO additions ranging from 0·1 to 10 wt% to ceramic $BaTiO_3$ have been studied. By means of a controlled processing, two different compounds were tested as a source of ZnO. The dopant distribution plays a key role in the microstructural development of the ZnO-doped $BaTiO_3$. When zinc stearate was used, homogeneous fine-grained microstructure was obtained for 0·1 wt% of ZnO. However, high density was avoided by burn out of the long organic chain. When solid ZnO was used as dopant, homogeneous fine-grained microstructure and density values around 99% D_t (D_t = 6·017 g cm^{-3}) were obtained for ZnO compositions starting from 0·5 wt%. The sintering temperature was 100°C lower than for undoped $BaTiO_3$. Control of grain growth in a wide temperature range led to ceramics with permittivity values close to 3000 and dielectric losses well below 1%. The incorporation of Zn^{2+} cations into the $BaTiO_3$ lattice takes place in Ba^{2+} sites, i.e. as an isovalent dopant. The solid solubility of ZnO in $BaTiO_3$ was stated to fall below 0·5 wt% in the range of sintering temperatures studied. Additions of large amounts of ZnO led to $BaTiO_3$–ZnO composite materials.

1 Introduction

Barium titanate based materials are widely used as a dielectric medium for manufacture of multilayer ceramic capacitors (MLCCs). Dielectric compositions with permittivity between 1000 and 3000 and X7R specifications (15% maximum capacity change between −55 and 125°C) contain around 90–98% of $BaTiO_3$. At present, these devices are greatly appreciated because of their high volumetric capacitive efficiency. However, ceramic capacitors can be up to three times more expensive than Al–Ta ones, and nominal capacity tolerances as high as 20% are usually specified. Moreover, as miniaturization of electronic circuits continues, higher volumetric efficiency is needed.[1–3]

This further improvement of the electrical properties is related to the ability to control the microstructural development of the ceramic. The presence of large $BaTiO_3$ grains decreases the dielectric constant, while interconnected porosity and secondary phases increase the value of dielectric losses. Microstructural homogeneity is also a critical feature since it determines the reliability of the ceramic material.[4] Heterogeneous microstructure can produce unpredictable properties, which obviously is related to the previously mentioned high value of tolerances. Furthermore, microstructural homogeneity can become a basic factor reducing the thickness of the dielectric ceramic layer in MLCC devices.

On the other hand, reduction of production costs depends mostly on the sintering temperature of the ceramic. During the fabrication of MLCC devices, dielectric ceramic and metallic inner electrodes are co-sintered.[2] In order to preserve the dielectric characteristics of the ceramic, reaction and/or diffusion between the ceramic and the electrode must be avoided. As a consequence, expensive noble metal alloys with high melting point have to be used, which greatly increases the production costs.

Dopant additions to $BaTiO_3$ decrease the sintering temperature and result in adequate dielectric properties of the material to the required specifications. A great number of papers have been devoted to the study of the role played by the additions of different oxides. However, a good understanding of many of the chemical and physical mechanisms

*Present address. Department of Materials Science & Engineering, Massachusetts Institute of Technology, 77 Massachusetts Avenue, Cambridge, MA 02139, USA.
† To whom correspondence should be addressed.

involved in microstructural development is still lacking. It is not uncommon to find contradictory data reported in the literature related to specific dopant additions.

ZnO additions to ceramic $BaTiO_3$ are reported to decrease the value of the loss tangent and increase the density of the sintered body. These results reveal that ZnO doping could be very interesting for $BaTiO_3$ based dielectric materials for high-quality capacitors. However, its effect on the sintering temperature, microstructure and dielectric constant is less clear. The Zn^{2+} cation has been considered as both an isovalent[5] and an acceptor[6] dopant in the $BaTiO_3$ lattice. Jaffe *et al.*[6] reported a solid solution limit of 0·7 wt% at 1200°C for ZnO in $BaTiO_3$. Swilam and Gadalla[7] found that ZnO additions above this limit drive the ceramic $BaTiO_3$ to higher densities, while the microstructure revealed the presence of a secondary liquid phase. More recently, Yoon *et al.*[8] reported a density increase of the ceramic $BaTiO_3$ for additions smaller than 0·1 wt%, but large grains were detected in the microstructure. Different impurity levels of the raw materials and the lack of control over the ceramic processing could be reasons for the observed differences in these materials.

The aim of the present work was to determine the effect caused by ZnO additions on the microstructural characteristics and electrical properties of the ceramic $BaTiO_3$, separating this effect from processing-related ones. For this purpose, doped and undoped samples were prepared by means of the same controlled processing and two different zinc compounds were tested as ZnO sources.

2 Experimental Procedure

$BaTiO_3$ raw material was a commercial grade (Rhône Poulenc s.A., ELMIC BT100) with Ba/Ti = 1·000, average particle size of 0·84 μm and specific surface of 2·7 $m^2\ g^{-1}$. The main impurity detected is Sr < 0·05 wt%. Two different compounds were chosen as zinc source: ZnO (Merck 8849) and $C_{36}H_{70}O_4Zn$ (zinc stearate; Merck 8865). The former shows an average particle size of 2·3 μm and the main impurity is SO_4^{2-} < 0·01 wt%. Zinc stearate has a density of 8·13/100 g cm^{-3} and after calcination leaves a ZnO solid residue of 14·3 wt%, assuming that all the zinc remains as ZnO.

Compositions with 0·1, 0·2, 0·5, 1, 5 and 10 wt% of ZnO were prepared by incorporating the appropriate amounts of zinc oxide or stearate to a dispersion of $BaTiO_3$ in isopropyl alcohol. Dispersion was attained by vigorous stirring by means of a high-speed turbine (6000 rev min^{-1}). Stirring was kept on during incorporation of the zinc compound to the dispersion. This step can modify the characteristics of the ceramic powder, by contributing to break powder agglomerates. Therefore undoped barium titanate was also dispersed in the same way, although no zinc compound was added. This allowed us to compare directly doped and undoped samples and separate different processing effects. After the mixing step, the powders were oven-dried (<100°C) and then sieved. A second set of zinc stearate doped powder was calcined at 500°C to burn out the organic chain. These powders were ground and sieved again.

Isopressed bars were obtained with 200 MPa pressure. Sintering was carried out in air, with heating and cooling rates of 3°C min^{-1}. Density of sintered samples was determined by the immersion method. Crystalline phases were determined by X-ray diffraction (XRD; Siemens D5000) and lattice parameters were measured by powder XRD, using internal standard and scanning rates of 0·5° 2θ min^{-1}. Microstructure was observed by scanning electron microscopy (SEM; Zeiss DSM 950) and transmission electron microscopy (TEM; Jeol 2000FX). Discs were sliced from the sintered bars for electrical characterization. Ag–Pd paste was used as electrode for measuring dielectric and losses constants, Curie temperature and electrical conductivity by complex impedance spectroscopy for 5 Hz–10 MHz frequency range in a Vectory Impedance Analyzer HP 4192A.

3 Results and Discussion

3.1 Sintering and microstructure

Density values as a function of sintering temperature for undoped $BaTiO_3$ (BT) are shown in Fig. 1.

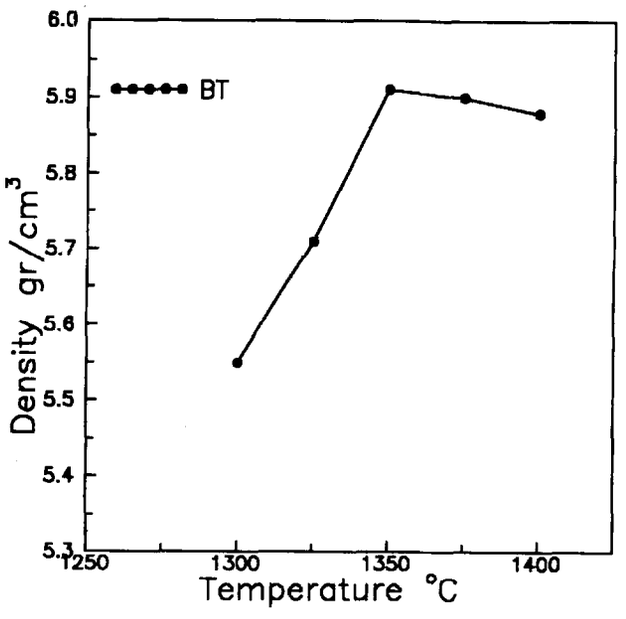

Fig. 1. Density versus sintering temperature for undoped $BaTiO_3$ (BT).

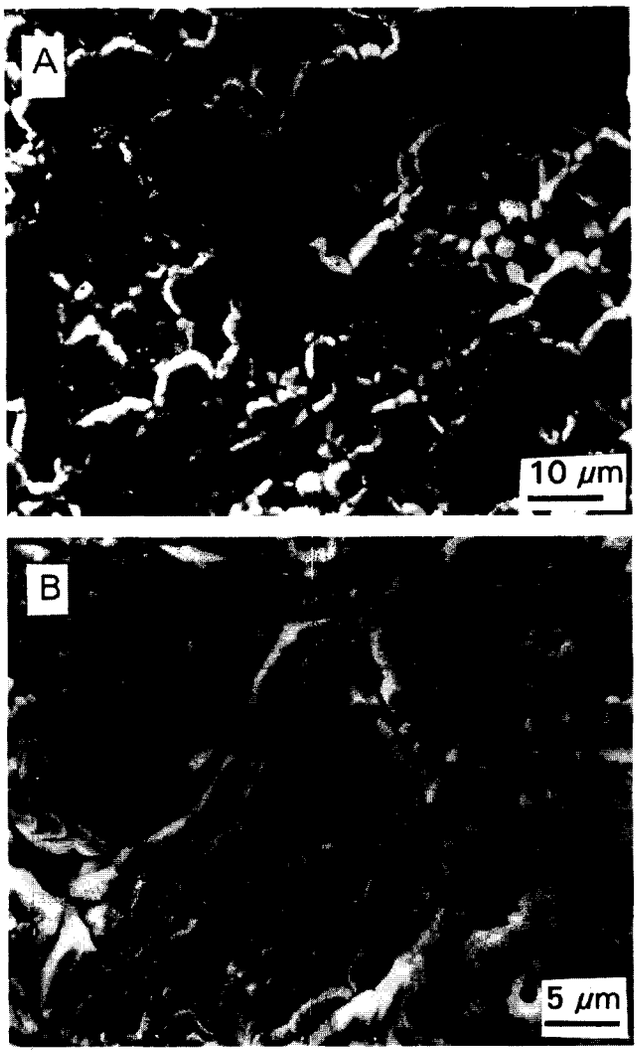

Fig. 2. SEM micrographs of BT sample sintered at 1350°C showing (A) fine-grained regions and (B) coarse grains.

The curve shows a rapid increase of density for sintering temperatures up to 1350°C, where the density reaches a maximum value around 98% D_t (D_t = theoretical density = 6·017 g cm^{-3}). For higher sintering temperatures, the apparent density value decreases slowly up to the sintering temperature of 1400°C. SEM study of the microstructure of BT samples revealed that sintering took place without grain growth control. In the samples sintered at lower temperatures fine-grained areas are observed together with coarse grains (Fig. 2). Increasing the sintering temperature made the fine-grained regions disappear, leading to grain sizes larger than 100 μm. On the other hand, SEM images did not reveal any liquid phase even for high sintering temperatures. This seems to indicate that solid-state diffusion is the main sintering mechanism. The morphology of the grains also suggests this mechanism. Nevertheless, it is well known that small amounts of liquid phases (located at some triple points or forming a thin layer between the grains) may not be detected by SEM.

In order to simplify the following discussion, the different ZnO-doped $BaTiO_3$ materials will be denoted as follows: Z if doped with solid ZnO, S if doped with zinc stearate and SC if doped with zinc stearate and calcined before sintering. Figure 3 shows the density values as a function of sintering temperature for all the ZnO-doped materials containing up to 1 wt% of ZnO. The density values are quite similar for all the samples doped with 0·1 wt% of ZnO. However, when the amount of ZnO increases, the behaviour of the different doped samples changes dramatically. Samples Z show high densities for a sintering temperature of 1250°C, 100°C less than that for undoped $BaTiO_3$. Furthermore, at sintering temperatures between 1300 and 1350°C, Z samples reached an apparent density value close to 99% D_t. On the other hand, the density of S and SC samples became lower when the amount of ZnO was increased.

3.1.1 Zinc stearate doped $BaTiO_3$

Homogeneous fine-grained microstructure is observed in S samples for all the cases (not shown). No secondary phases were detected. The addition of 0·1 wt% of ZnO drives the material to high density without the anomalous grain growth observed in the undoped BT materials. The reason for such a high efficiency of the ZnO may be related to its good distribution. Assuming that zinc stearate adsorbs on the surface of the $BaTiO_3$ particles in a similar way to that reported for phosphor stearate additions,[9] the ZnO would be well distributed along the surface of the $BaTiO_3$ particles. This modification of the surface could be the origin of the grain growth control.[10] Further discussion of this point is beyond the scope of the present work and will be addressed in a following paper. The fall in density when the amount of ZnO is increased is related to the nature of the stearate compound. High density values are avoided by the presence of large pores and interconnected porosity channels. The origin of these large voids is the agglomeration state of the powders given by the organic. During the sintering step, a large volume of CO and/or CO_2 gases is generated inside the ceramic compact which leaves voids on its way out of the ceramic. Obviously, this effect increases with the amount of stearate incorporated and, in the case of the sample containing 1 wt% of ZnO, causes catastrophic cracking of the sample.

From the above discussion it follows that homogeneous fine-grained microstructure and high density are expected in the samples SC, since the doped powder was calcined before the green compacts were obtained. Certainly, the density of the SC materials is higher than that of the S ones

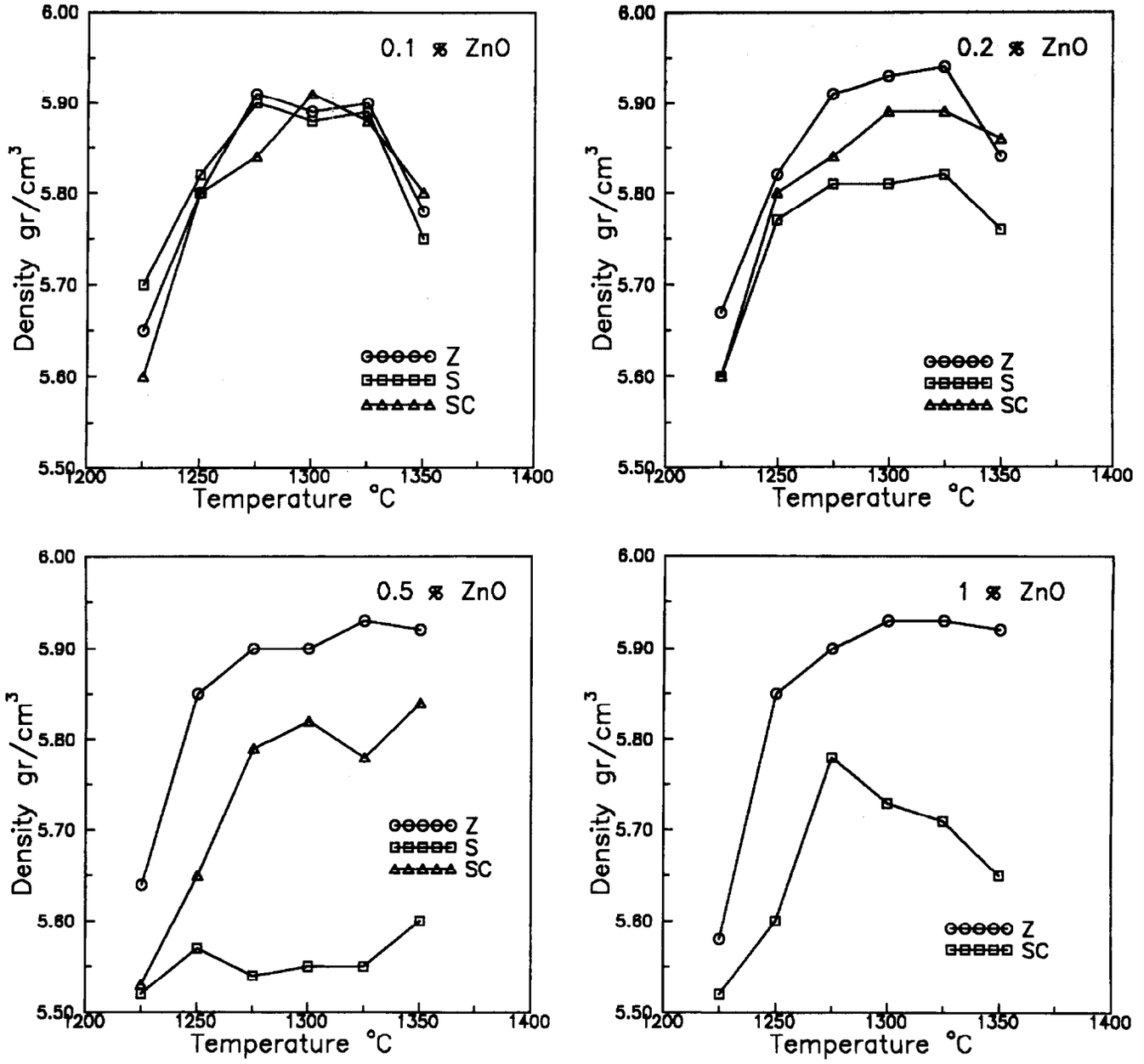

Fig. 3. Density versus sintering temperature for ZnO-doped materials containing up to 1 wt% ZnO.

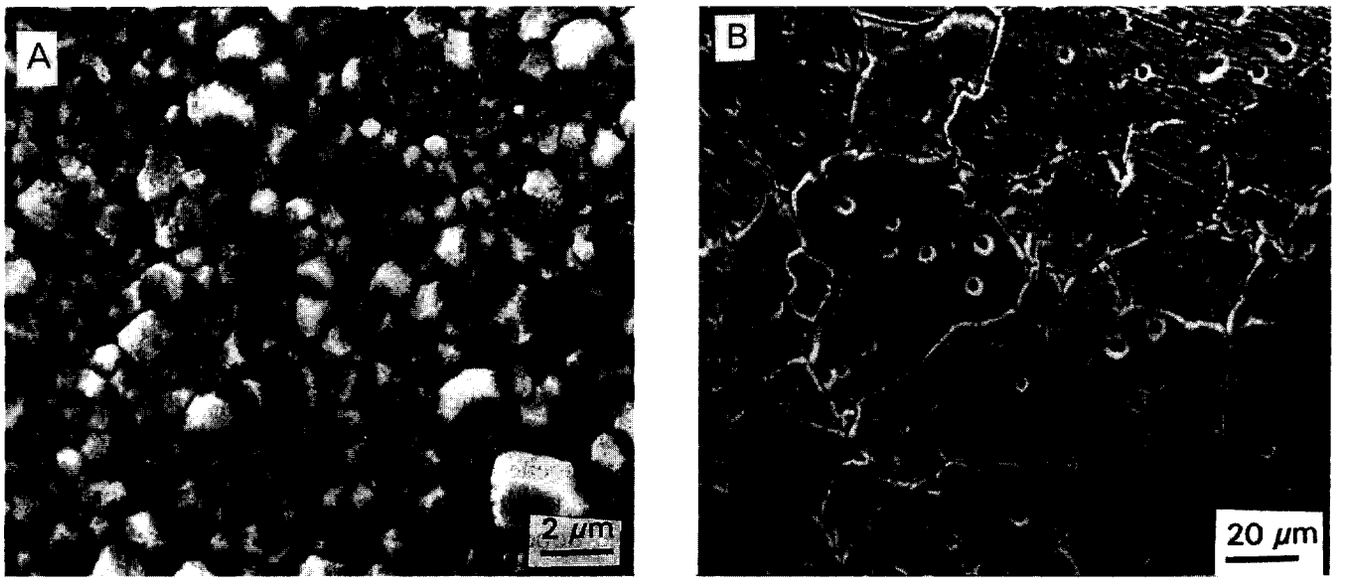

Fig. 4. SEM micrographs of SC sample doped with 0·1 wt% of ZnO sintered at 1300°C (A) fine-grained area and (B) coarse grains.

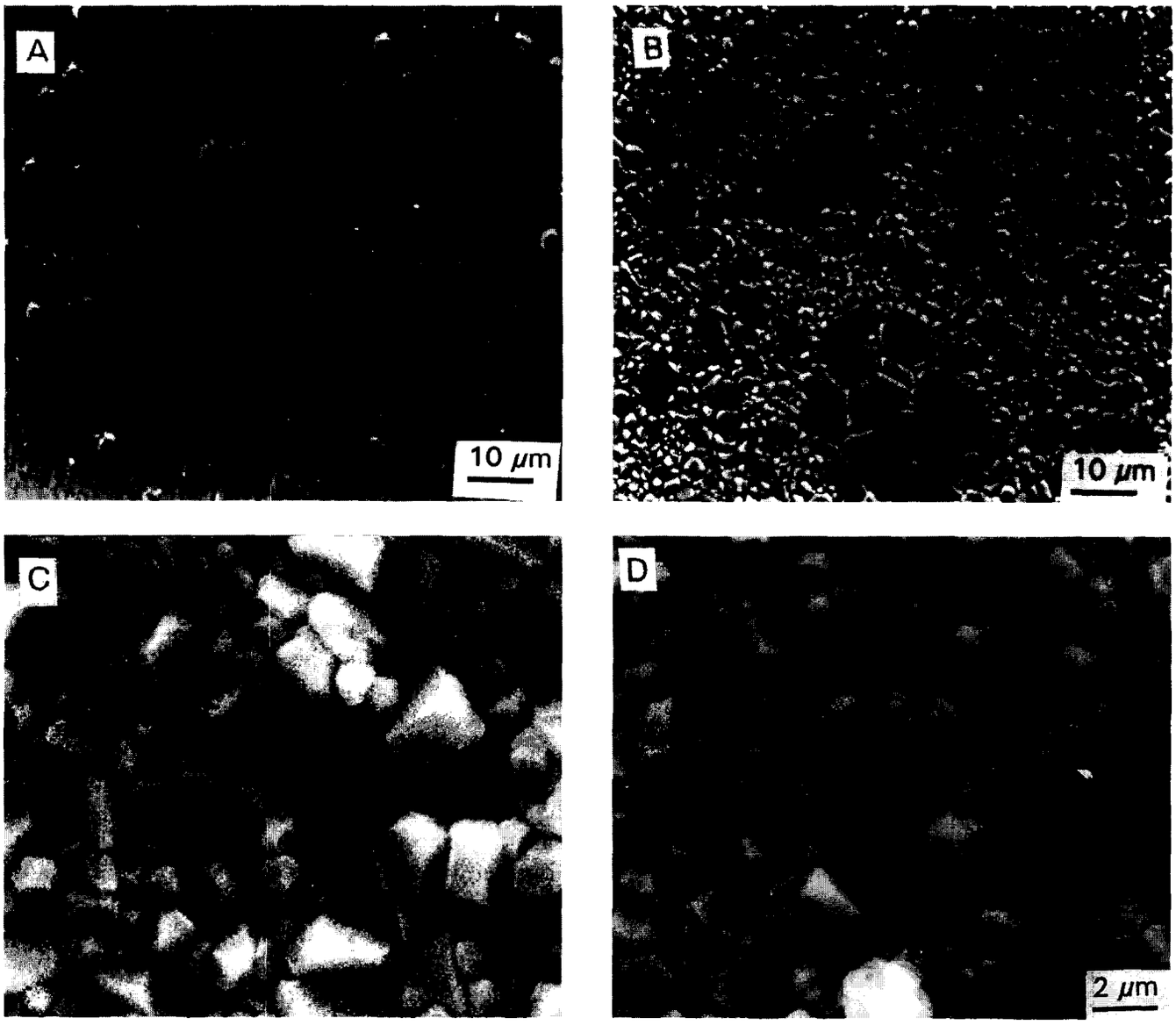

Fig. 5. SEM micrographs of Z samples sintered at 1300°C for ZnO amounts of (A) 0·1%, (B) 0·2%, (C) 0·5% and (D) 1%.

but still lower than for Z materials. On the other hand, the microstructure (Fig. 4) reveals coarse-grained areas in a matrix of fine grains. In this case this behaviour is related to the different processing. The burnout step modified the morphology of the doped ceramic powder and gave rise to the presence of strong agglomerates which remained after grinding and re-sieving the powder. These agglomerates cause anomalous grain growth during the sintering of the material.[11]

3.1.2 Zinc oxide doped $BaTiO_3$

SEM micrographs of Z materials sintered at 1300°C are shown in Fig. 5. For the materials doped with 0·1 and 0·2 wt% of ZnO, regions with large grains are detected together with fine grains. The samples doped with 0·5 and 1 wt% of ZnO show a homogeneous fine-grained microstructure. By comparison with the observed microstructure of the S sample with 0·1 wt% of ZnO, it seems that processing-related effects are reflected in the Z materials doped with 0·1 and 0·2 wt% of ZnO. Taking into account the doping process, after the mixing step the doped ceramic powder is composed of large particles of solid ZnO, each of them surrounded by more than 1000 $BaTiO_3$ particles. This means that the ZnO distribution is less effective than for the S materials. During the sintering some $BaTiO_3$ particles do not 'see' the ZnO particles and behave like the undoped BT material. However, when the amount of dopant is increased, the material reaches the same fine-grained microstructure as that of the S sample with 0·1 wt% of ZnO. Note that, as a consequence of a worse ZnO distribution, a larger amount of dopant is needed to obtain the same effect on the material.

Another remarkable result is the stability of the microstructure with sintering temperature for these materials. Samples Z with ZnO additions equal to or larger than 0·5 wt% of ZnO can be sintered to high density (98–99% D_t) for a wide

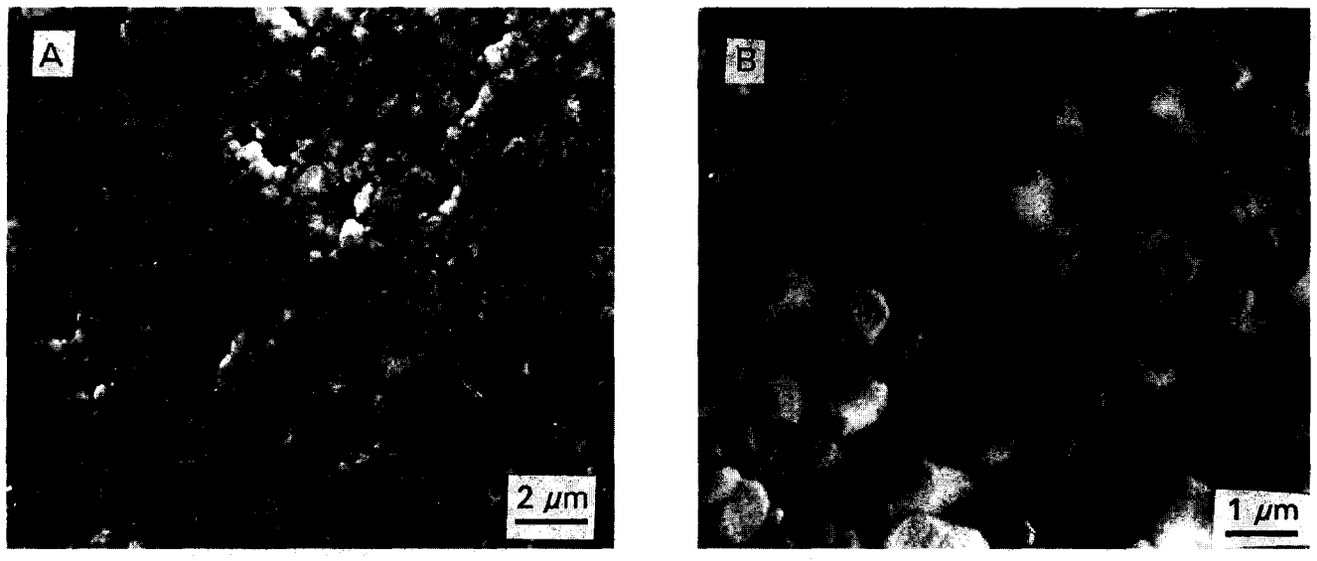

Fig. 6. SEM micrographs of Z samples doped with 0·5 wt% of ZnO sintered at (A) 1250°C and (B) 1350°C.

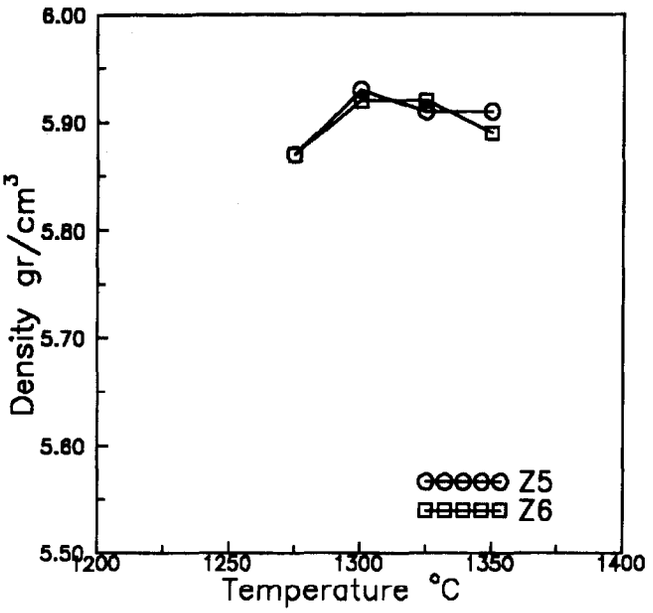

Fig. 7. Density versus sintering temperature for Z samples doped with 5 and 10 wt% of ZnO.

range of temperatures. For the sample containing 0·5 wt% of ZnO, high density and homogeneous fine-grained microstructure are obtained between 1250 and 1350°C (Fig. 6). This 100°C range for sintering temperatures is unusual for $BaTiO_3$ materials (and it may be even larger since higher temperatures were not tested). As in the case of the undoped BT, neither SEM nor TEM studies revealed any evidence of liquid phase formation for the Z samples even at sintering temperatures as high as 1350°C. This result, together with the rounded shape of the grains, points to a sintering process by volume diffusion.

Samples doped with ZnO percentages higher than 1 wt% show important differences. Density is still high (around 98% D_t) for sintering temperatures ranging from 1275 to 1350°C (Fig. 7). However, the microstructure shows the presence of large ZnO grains surrounded by small grains of $BaTiO_3$ (Fig. 8). The behaviour of the matrix of $BaTiO_3$ grains (regarding the sintering temperature)

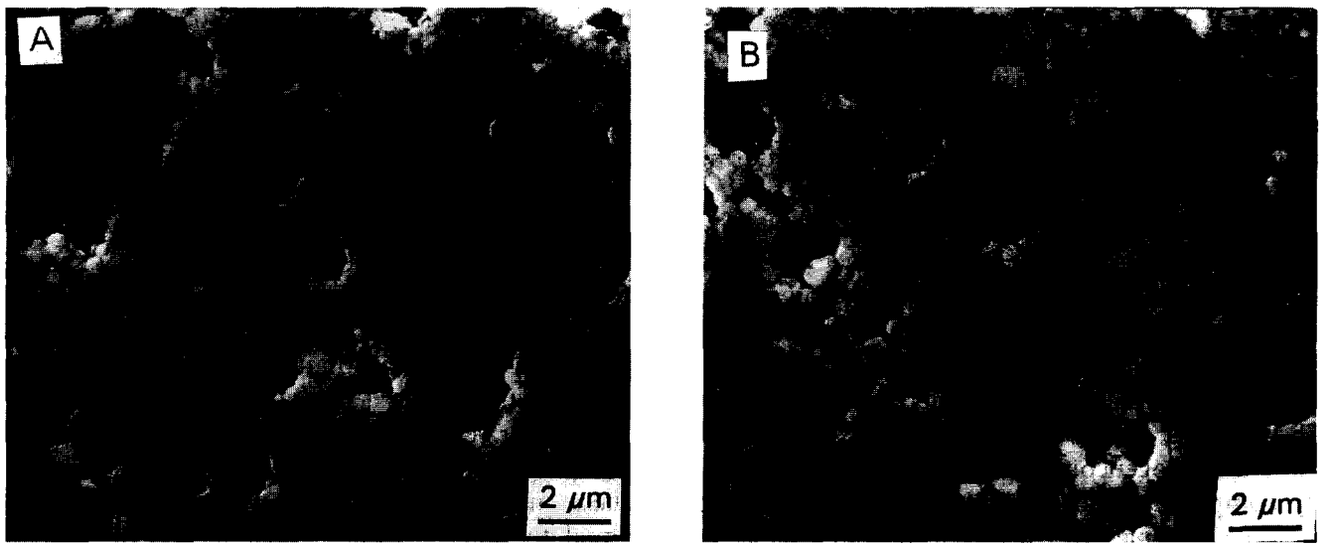

Fig. 8. SEM micrographs of Z samples sintered at 1300°C with ZnO amounts of (A) 5% and (B) 10%.

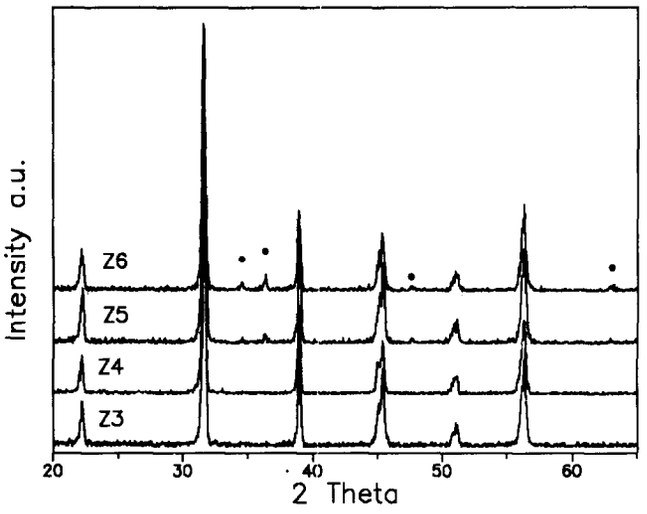

Fig. 9. XRD patterns of Z samples sintered at 1300°C and containing from 0·5 to 10 wt% of ZnO. Marked peaks belong to ZnO.

is the same as that of the Z materials with 0·5 or 1 wt% of ZnO. No liquid phase was detected in these samples for the range of temperatures studied.

3.1.3 XRD analysis

Figure 9 shows the diffraction patterns of the Z samples sintered at 1300°C and containing 0·5, 1, 5 and 10 wt% of ZnO. ZnO peaks are clearly detected for the samples with larger amounts of ZnO. However, the presence of ZnO grains in the samples with lower amounts of ZnO cannot be discarded in view of these results; obviously 0·5 wt% of crystalline ZnO falls below the detection limit of this technique. On the other hand, although study of the microstructure did not reveal the presence of ZnO grains in these materials, it is possible that a certain number of small ZnO grains remain undetected. Such low ZnO concentration may be very difficult to detect if it is well distributed all around the sample.

The $BaTiO_3$ lattice parameters and tetragonality measured by XRD are represented in Fig. 10. Both parameters *c* and *a* change for ZnO additions up to 0·5 wt% and remain unchanged for higher ZnO additions. This result indicates that Zn^{2+} is incorporated into the $BaTiO_3$ lattice. The change of the *c* parameter suggests that this incorporation takes place in the A sites of the perovskite. Otherwise, Zn^{2+} incorporation in the Ti^{4+} sites would cause an increase of the *c* parameter due to the larger size of the Zn^{2+}. On the other hand, the ilmenite structure of $ZnTiO_3$[12] indicates that the zinc cation is too small to support the perovskite structure. Therefore, low amount of Zn^{2+} is expected to be incorporated in A sites, which means that a low solid solution limit of ZnO in $BaTiO_3$ is expected. In fact, taking into account the limitation of the XRD measurements, it is possible to state that the solid solution limit is lower than 0·5 wt% of ZnO.

The characteristics of the microstructure also support the formulated hypothesis on the substituting of Zn^{2+} for Ba^{2+}. If Zn^{2+} replaces Ti^{4+}, an excess of TiO_2 should exsolve due to its low solubility in $BaTiO_3$.[13] As is well known, the TiO_2 excess initiates liquid phase formation for temperatures above the eutectic point in the system BaO–TiO_2. Furthermore, grain growth in $BaTiO_3$ is strongly promoted in the presence of TiO_2 excess. None of these effects have been observed, even for samples heavily doped and sintered well above the eutectic point of the system. Therefore, the incorporation of Zn^{2+} in A sites is completely coherent with the data obtained in this work.

3.2 Electrical properties

Table 1 shows the values of dielectric and losses constants measured at 1 kHz and room temperature for the undoped BT material. As a consequence of

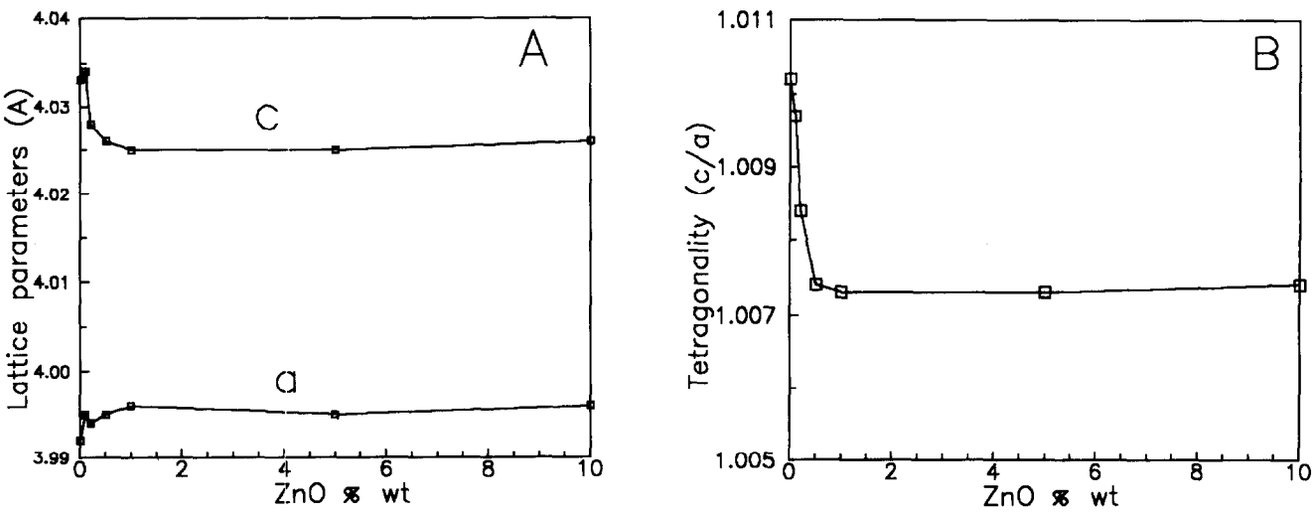

Fig. 10. Lattice parameters (A) and tetragonality (B) of Z materials sintered at 1300°C.

Table 1. Dielectric and losses constants for undoped BT

Sintering temperature (°C)	ϵ' f = *1 kHz*	*tg(δ)(%)* f = *1 kHz*
1300	3022	5·90
1325	2897	4·91
1350	3040	4·48
1375	2655	3·89
1400	2506	2·76

the grain growth, the dielectric constant decreases when the sintering temperature increases. However, these values are higher than expected according to the grain sizes detected. On the other hand, dielectric losses are also very high, even when the density reaches values around 98% D_t for sintering temperatures of 1350°C and above. The dependence of the dielectric constant on the temperature can be seen in Fig. 11. Undoped BT samples show the Curie temperature at 126°C.

As previously discussed, S samples showed extensive cracking which made reliable electrical characterization problematic. On the other hand, SC samples reflect strong processing-related effects which may be difficult to separate from the ZnO doping effects. Therefore, the electrical characteristics of the Z materials are the most adequate to be compared with those of the undoped BT (Fig. 11).

Table 2 shows the dielectric and losses constants measured for all the Z materials sintered at different temperatures. The dielectric constants of the materials containing 0·1 and 0·2 wt% of ZnO are more sensitive to sintering temperature because of the presence of large grains which grow when the sintering temperature is raised. In agreement with the high homogeneity of their microstructure, Z samples with 0·5 and 1 wt% of ZnO show very little change of the dielectric constant with sintering temperature. Higher additions of ZnO lead to two-phase material, hence the dielectric constant falls below the values measured for the rest of the samples. More spectacular is the reduction of the dielectric losses. In all cases these losses have been diminished by about one order of magnitude with respect to the undoped barium titanate. This effect was registered for the whole range of sintering temperatures studied. By comparing with the undoped materials, the lower dielectric losses cannot be due to the high density. Doped and undoped samples with almost the same density value show one order of magnitude difference between their loss tangent values. Therefore, it seems that ZnO additions may cause a lower conductivity in the material.

The Curie temperature is 119°C (7°C less than that of undoped BT) for the Z samples doped with up to 1 wt% of ZnO. For the sample doped with 5 wt% of ZnO, the Curie temperature detected is 122°C (4°C lower than that of undoped BT). The shift of the Curie temperature reflects the incorporation of zinc cations into the $BaTiO_3$ lattice. On the other hand, the shape of the peaks is a consequence of the fine-grained microstructure. No relevant variations were detected for the samples sintered at different temperatures. The behaviour of these curves indicates that incorporation of Zn^{2+} into the $BaTiO_3$ lattice has already taken place for samples sintered at the lowest temperatures, while the amount of ZnO incorporated as solid solution seems to be unchanged (or changes very slightly so that it is not detected) for different sintering temperatures.

3.2.1 Complex impedance spectroscopy

Impedance diagrams of doped and undoped samples

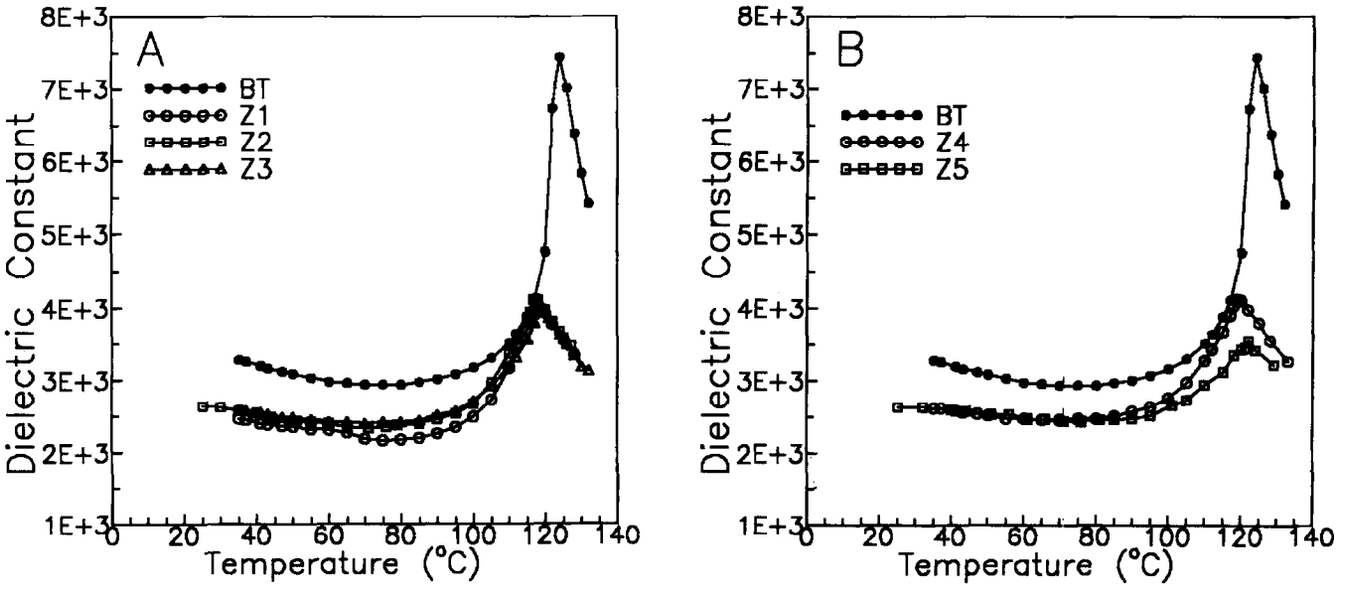

Fig. 11. Dielectric constant versus temperature for Z materials sintered at 1300°C.

Table 2. Dielectric and losses constants for Z materials

	Z1		*Z2*		*Z3*		*Z4*		*Z5*		*Z6*	
T(°C)	ϵ'	$tg\delta$	ϵ'	$tg\delta$	ϵ'	$tg\delta$	ϵ'	$tg\delta$	ϵ'	$tg\delta$	ϵ'	$tg\delta$
1250	2719	1·00	3031	0·84	2809	0·38	2731	0·44	1934	0·35	2119	0·41
1275	2566	0·41	2756	0·43	2561	0·84	2596	0·35	2337	0·32	2028	0·61
1300	2081	0·28	2570	0·42	2706	0·46	2431	0·55	2002	0·62	1988	0·62
1325	1677	0·11	2457	0·42	2436	0·44	2572	0·40	2033	0·61	1700	0·53
1350	1233	0·34	2171	0·26	2576	0·43	2219	0·38	1941	0·27	1819	0·51

show important differences. Figure 12 shows the diagrams for undoped BT sintered at 1350°C and 0·5 wt% ZnO-doped material sintered at 1300°C. Both samples present comparable density values. Grain and grain boundary contributions are clearly shown for the undoped BT material; however, the Z materials, as a general feature, show strong overlapping of both contributions. Due to this overlapping, the grain contribution (much smaller than the grain boundary one) was not possible to analyse with reasonable accuracy. The origin of this behaviour of the doped samples is due to two main factors: high density of grain boundaries due to the fine-grained microstructure and strong decrease of the grain boundary conductivity.

Figure 13 shows a plot of grain boundary conductivity versus temperature for the Z materials sintered at 1300°C. The grain boundary conductivity of Z materials is about one order of magnitude lower than that of the undoped material, which seems to correlate well with the strong decrease of the dielectric losses. Heavily doped samples exhibit grain boundary conductivity somewhat higher. In these cases the grain boundary contribution is composed of boundaries with different characteristics as a consequence of the presence of considerable amount of ZnO grains. However, for Z samples doped with between 0·2 and 1 wt% of ZnO, the electrical characteristics of the grain boundaries are almost identical. Furthermore, these characteristics seem to be unchanged for the range of sintering temperatures studied (Fig. 14).

The change of the grain boundary characteristics with respect to the undoped BT material may be understood by taking into account the small solid solution limit of ZnO in $BaTiO_3$. Due to the size mismatch between Zn^{2+} and Ba^{2+}, progress of the solid solution towards grain interiors is not expected. If it is so, ZnO-rich grain boundaries and/or segregated ZnO at the interface between the grains is expected, which would be responsible for the change of the grain boundary characteristics. Nevertheless, more data are needed in order to clarify this point.

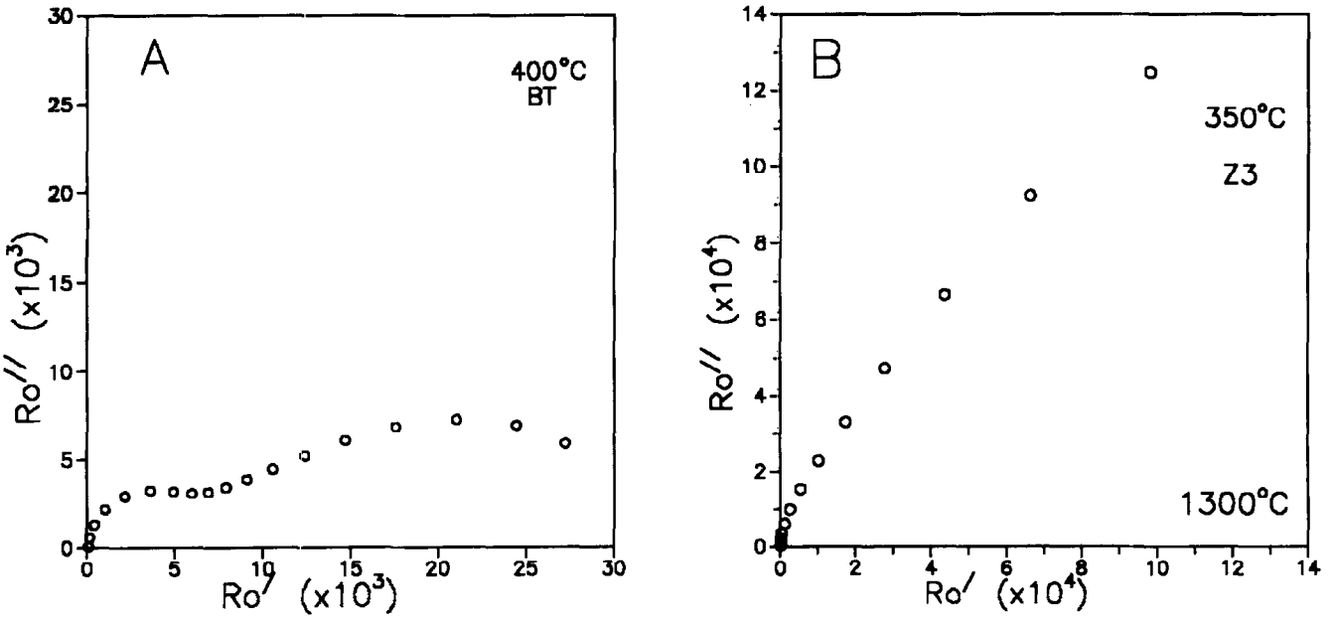

Fig. 12. Impedance diagrams of undoped BT sintered at 1350°C (A) and Z sample with 0·5 wt% of ZnO, sintered at 1300°C (B).

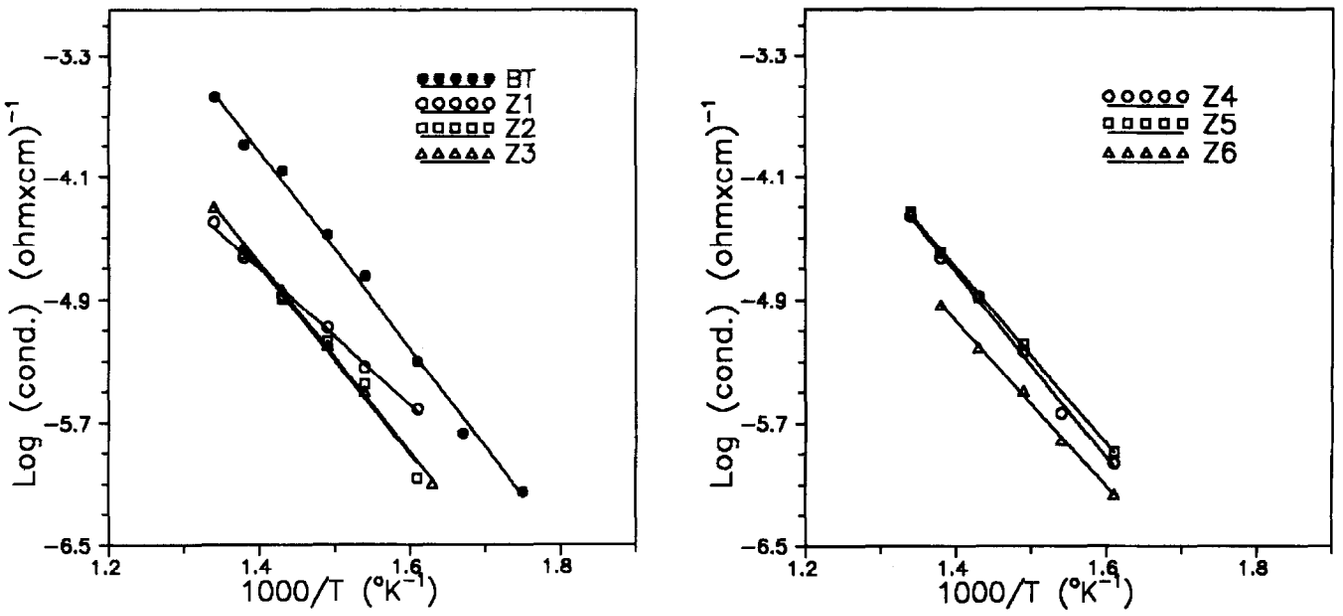

Fig. 13. Grain boundary conductivity versus temperature for undoped BT and Z materials sintered at 1300°C.

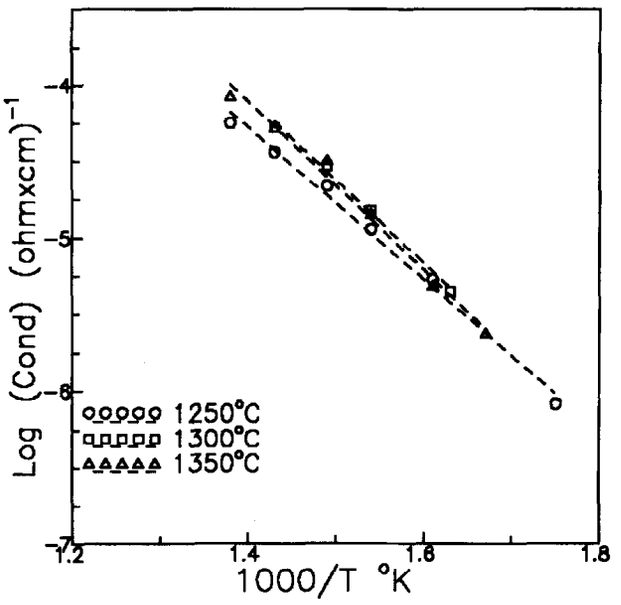

Fig. 14. Grain boundary conductivity versus temperature for Z samples containing 0·5 wt% of ZnO and sintered at different temperatures.

4 Conclusions

ZnO additions to ceramic $BaTiO_3$ have been studied in the present work. Two different compounds were tested as ZnO source: zinc stearate and solid ZnO. Materials doped with stearate show that ZnO additions of 1 wt% were able to control the grain growth and led to homogeneous fine-grained microstructures. However, as a consequence of the burnout of the long organic chain of the stearate, high density values were obtained only for low ZnO contents. On the other hand, if the doped powder is calcined before sintering in order to eliminate the organic chain, strong powder agglomeration takes place, driving heterogeneous microstructures of the sintered ceramics.

In the case of materials doped with solid ZnO, homogeneous fine-grained microstructures are obtained starting with ZnO amounts of 0·5 wt%. This difference with the stearate-doped material revealed that the ZnO distribution in the $BaTiO_3$ powder plays a critical role in the microstructure development. Z materials show density values as high as 99% D_t for sintering temperatures 100°C lower than for undoped material. High densities and homogeneous fine-grained microstructures were obtained for a 100°C wide range of sintering temperatures and for ZnO compositions between 0·5 and 1 wt%. ZnO amounts larger than 1 wt% gave rise to $BaTiO_3$–ZnO composite materials. The solid solution limit of ZnO in $BaTiO_3$ appears to fall below 0·5 wt% of ZnO in the range of temperatures studied.

Regarding the electrical characteristics of the ZnO-doped materials, several remarkable points have been observed. Dielectric constant values between 2000 and 3000 are measured for the ZnO-doped samples. These values remained stable, together with the microstructure of the material, for a wide range of sintering temperatures and different ZnO percentages. The dielectric losses were well below 1% for all the ZnO-doped materials studied, even for heavily doped samples which show two-phase microstructure composed of ZnO and $BaTiO_3$.

In view of these results, ZnO-doped $BaTiO_3$ compositions have excellent characteristics as dielectric materials for high-quality capacitors.

Furthermore, the results obtained for heavily doped samples are very interesting for the purpose of capacitor–varistor integration.

Acknowledgements

The authors would like to express their gratitude for the support of the Spanish Science Ministry (CICYT MAT94-807).

References

1. Goodman, G., Ceramic capacitor materials. In *Ceramic Materials for Electronics*. ed. R. C Buchanan. Marcel Dekker Inc., New York, 1986.
2. Khan, M., Burks, D. P., Burn, I. & Schulze, W. A., Ceramic capacitor technology. In *Electronic Ceramic Properties: Devices and Applications*, ed. L. M. Levinson. Marcel Dekker Inc., New York, 1988.
3. Sheppard, L., Progress continues in capacitor technology. *Am. Ceram. Soc. Bull.*, **72**[3] (1993) 45–47.
4. Artl, G., The influence of microstructure on the properties of ferroelectric ceramics. *Ferroelectrics*, **104** (1990) 217–227.
5. Baxter, P., Hellicar, N. J. & Lewis, B., Effect of additives of limited solid solution on ferroelectric properties of barium titanate ceramics. *J. Am. Ceram. Soc.*, **42**[10] (1959) 465–470.
6. Jaffe, B., Cook, W. R. & Jaffe, H., *Piezoelectric Ceramics*. Academic Press, London–New York, 1971.
7. Swillam, M. N. & Gadalla, A. M., Effect of additions on the sinterability of barium titanate. *J. Trans. Br. Ceram.*, **74**[5] (1975) 165–169.
8. Yoon, K. H., Kim, J. W. & Jo, K. H., Dielectric properties of $BaTiO_3$ with Sb_2O_3 and ZnO. *J Mater. Sci. Lett.*, **8** (1989) 153–156.
9. Caballero, A. C., Fernández, J. F., Durán, P. & Moure, C., Phosphor-doped $BaTiO_3$: microstructure development and dielectric properties. *J. Mater. Sci.*, **30** (1995) 3799–3804.
10. Fernández, J. F., Caballero, A. C., Durán, P. & Moure, C., Improving sintering behaviour of $BaTiO_3$ by small doping additions. *J. Mater. Sci.*, **31** (1996) 975–981.
11. Yan, M. F., Effect of physical, chemical and kinetic factors on ceramic sintering. *Adv. Ceram.*, **21** (1987) 635–669.
12. Dulin, F. H. & Rase, D. E., Phase equilibria in the system ZnO–TiO_2. *J. Am. Ceram. Soc.*, **43**[3] (1960) 125–131.
13. Sharma, R. H., Chan, N. H. & Smyth, D. M., Solubility of TiO_2 in $BaTiO_3$. *J. Am. Ceram. Soc.*, **64** (1981) 448–451